# Demonstration of spectral calibration for stellar interferometry

Richard T. Demers, Xin An, Hong Tang, Mayer Rud, Leonard Wayne, Andrew Kissil and Eug-Yun Kwack

Jet Propulsion Laboratory, California Institute of Technology,
4800 Oak Grove Dr, m/s 171-113
Pasadena, CA91109
818 393 0474
richard.t.demers@jpl.nasa.gov

**ABSTRACT**

A breadboard is under development to demonstrate the calibration of spectral errors in microarcsecond stellar interferometers. Analysis shows that thermally and mechanically stable hardware in addition to careful optical design can reduce the wavelength dependent error to tens of nanometers. Calibration of the hardware can further reduce the error to the level of picometers. The results of thermal, mechanical and optical analysis supporting the breadboard design will be shown.

## 1. INTRODUCTION

The Spectral Calibration Development Unit (SCDU) is a breadboard of the SIM (Space Interferomatery Mission) PlanetQuest astrometric beam combiner developed by the NASA Jet Propulsion Laboratory. SCDU is specifically designed to develop wavelength calibration methodology through extensive automated test and measurement. SCDU encompasses nearly all major components of the SIM astrometric beam combiner including a star tracker, fringe sensor, siderostats, metrology, retro-source and beam combining optics The optical beam train will consist of two interferometric arms of equal length and configuration. The two arms are combined at the main beam splitter (MBS) in order to interfere the beams from the two arms and produce a fringe on the Fringe Tracking (FT) camera. The beam downstream from the MBS is referred to as “combined space” or “common mode space”. Conversely, the part of the beam train upstream from the MBS (the separate interferometer arms) is referred to as “non-common mode space”.

In its initial configuration SCDU will be operated exclusively in retro-mode whereby both a white light source (450-950nm) and a metrology source (1.314nm) will be introduced internally in combined space by two fibers and collimators and propagated out to the two arms and retro-reflected back to the beam combining optics and fringe sensor. The retro mirrors, called siderostats (SID), each consist of an annular mirror of outer diameter 41 mm and inner diameter 25 mm to reflect white light. A gold coated corner cube mounted in the annular hole of each SID retro-reflects the metrology pencil beams. The arms of the interferometer are equal in length by design. The slight inequality in path lengths due to placement error is mitigated by a translation stage on one of the SIDs. Each of the arms will also contain Voice-Coil-Modulators (VCMs). In a typical observation, the path length of one arm of the interferometer will be modulated by a triangle wave with 50 Hz duty cycle via the VCM of that arm. The resulting modulated fringe will be recorded by the FT. The measurement of the modulated fringe using a retro-mode source is a simulation of the starlight observation that will be made by SIM. Two servo control loops will operate during observations. The star tracker will sense tilt errors due to vibration and thermal distortion and will apply corrections through the SID pointing. The fringe camera will be used to sense fringe drift and will correct by displacing the motion center of the VCM.

The recorded fringe measurements will be calibrated in post processing by a mathematical algorithm. In order to test and refine this algorithm, a large number of fringe measurements will be carried out in vacuum. Measurements will be taken over short periods of approximately 24 minutes and long periods up to 90 minutes. Automated alignment will be carried out periodically. The high volume of measurements will be done efficiently using software automation.

## 2. OJBECTIVES AND REQUIREMENTS

The Spectral Calibration Development Unit is fundamentally intended to demonstrate wavelength calibration accuracy and stability between sources of different color and polarization. SCDU must sense and calibrate over the range from 450 to 950 nm. Spectral energy densities (SEDs) from F, G, K and M stars will be simulated on the breadboard.

To be successful SCDU must demonstrate a wavelength calibration procedure that is both accurate and stable enough to meet the SIM astrometric error budget. The white light fringe error of SCDU for narrow angle observations must not exceed 4 picometers. A related requirement is that of the static dispersion of the optical system. In single pass SCDU must have a peak to valley static dispersion that does not exceed 30 nm. (The design goal is actually far smaller.) In a single instrument pass the light travels from the source to the SIDs. Since SCDU will be operated in retro-reflection mode light travels from the retro source (located in the combined optical space) to the SIDs and makes a return pass to the conbined space. We thus say that SCDU is a double pass interferometer. SCDU must also demonstrate picometer level requirements for performance of metrology and alignment and wavefront stability.

Many sources are partially linearly polarized. The optical system itself has a polarization dependent response. For example, mirrors with metallic coatings will impose different phase shifts for ‘p’ and ‘s’ polarized light. For linearly polarized input, the instrument will produce two separate fringes, one for each orthogonal polarization. The two fringes will have a mutual phase retardance due to the different phase responses. The requirement for SCDU is that for a 1% polarized source the instrument retardance must not exceed 1 picometer.

Since wavelength calibration is a field independent quantity, it is not necessary for SCDU to simulate the field dependent operation associated with the angular displacement of siderostats. Nor will an external pseudostar be needed. Stellar sources of different spectral energy distribution will be simulated by placing color filters in front of the white light retro source.

## 3. STRUCTURE

SCDU is being built on a custom optical bench (10.5 x 6.7 x 1 ft) previously used for the SIM Micro-arcsecond Metrology Testbed[1] (MAM). It was found that this bench did not have adequate stiffness. Consequently, for SCDU, this large bench will be used to support only the optics whose stability requirements are not the most demanding. To attain the required stability of the beam combiner core optics and control loop sensors a mechanically stiff sub-bench ( 6.5 x 4 x 0.53 ft) will be kinematically mounted on the large bench. The sub-bench has super invar face sheets with an aluminum honeycomb core. The entire system will be supported on three fixed points by a truss support. The entire opto-mechanical breadboard will be operated in a large vacuum chamber situated in a class 10,000 temperature controlled clean room.

Structural and thermal analysis was carried out to predict the dynamic behavior and thermal stability of the system in vacuum testing. A finite element model of the optical bench system was constructed to predict the dynamics and thermal drift of the optics. The FEM included the structure of the bench, sub-bench and simplified models of the opto-mechanical mounts. The analysis was carried out as follows. First all heat sources (e.g. actuators, stepper motors) and sinks (CCD camera cooling lines) on the optical bench were turned on with constant temperature outside the vacuum chamber and the system was allowed to reach thermal

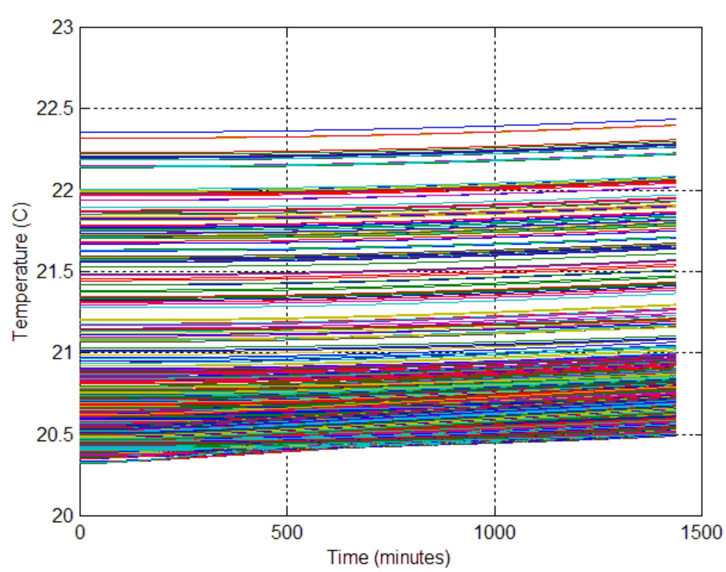


**Figure 1.** Temporal temperature profile of a series of nodes on the optical bench resulting from FEM analysis.

equilibrium. The resulting spatial temperature profiles were used as the initial condition for the system when an external stimulus was applied. The external stimulus was a 1° C step function increase in the ambient temperature outside the vacuum chamber. The 1° C instantaneous increase was based on observations of the laboratory temperature over a one year period and was intended to provide an upper bound on thermal drift inside the vacuum chamber. The resulting temporal temperature profiles were used as inputs to the structural FEM to determine the temporal profiles of three dimensional translations and rotations of many optical nodes. The temporal temperature profiles over a 24 hour period are shown in Figure 1. The temporal profiles of the largest displacements in translations and rotations are shown in Figures 2 and 3, respectively.

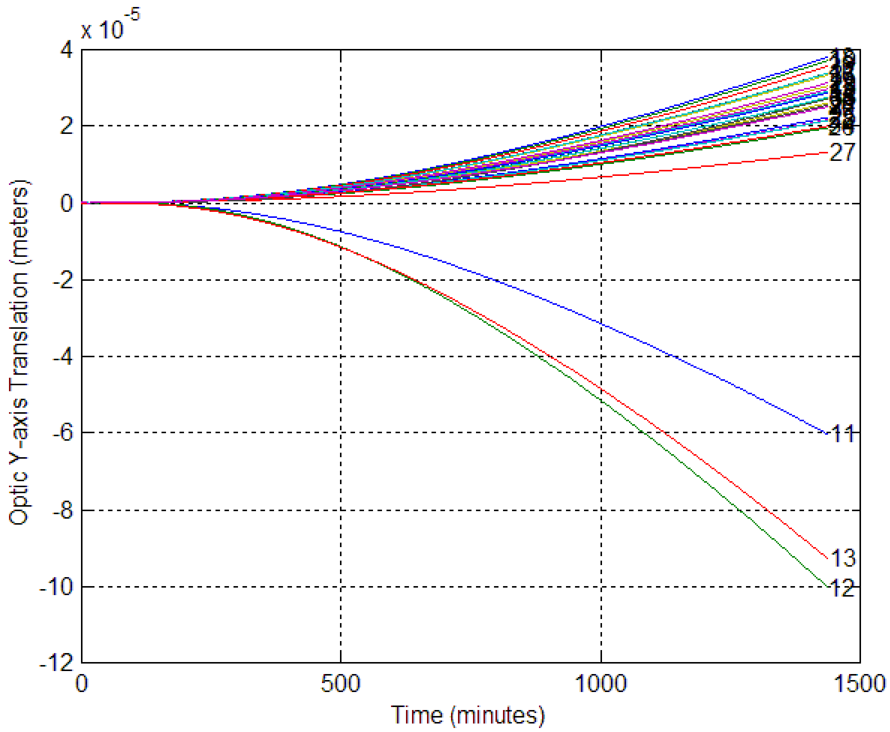


**Figure 2.** Temporal temperature profile of the Y axis translation of a number of optics on the sub-bench resulting from a 1° C external stimulus.

The analysis predicts that the highest rate of change of linear displacement due to thermal drift occurs for optic node number 12 whose drift in the Y-direction is approximately 3 microns per half hour (Figure 2). The worst case of thermally induced rotational displacement is predicted for optic node number 13 whose angular velocity about the X axis is less than 70 nanoradians over one half hour (Figure 3).

## 4. COMBINER ARCHITECTURE

The optical layout of SCDU is shown in Figure 4. The pair of SIDs and voice coil modulators (VCMs) appear in the lower left and lower right corners, respectively. The super invar sub-bench is located in the top half of the view and contains all of the core optics comprising the beam combiner as well as the retro-mode white light source and metrology beam launcher. The white light source is launched by a fiber located in the figure near the lower edge of the sub-bench, denoted by X4. The metrology beam launcher is located near the center of the sub-bench (X1); angle tracking camera is near the top (X29); fringe tracking camera is located at the left of the sub-bench (X44).

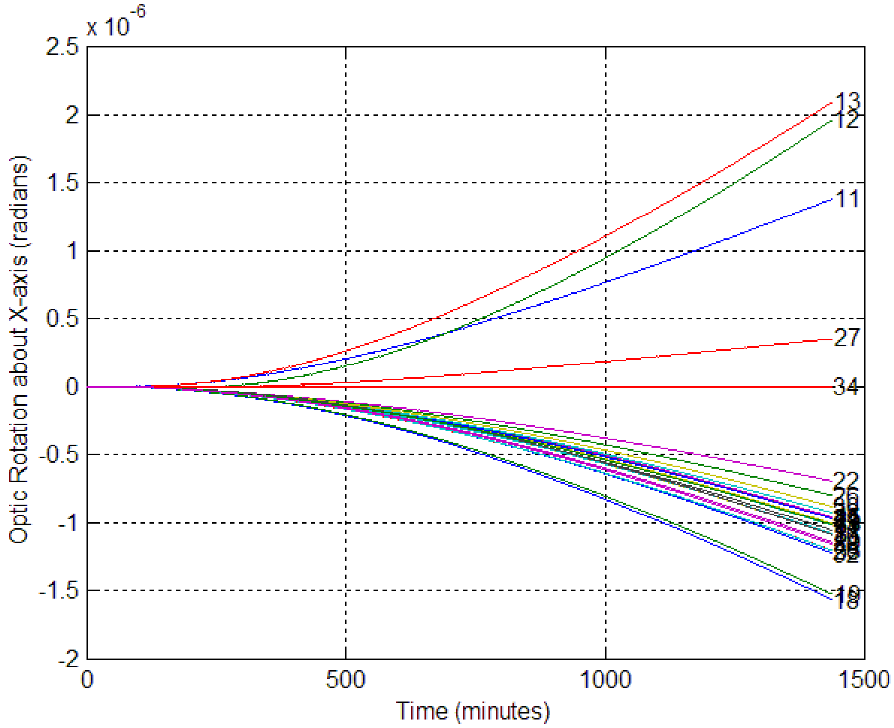


**Figure 3.** Temporal temperature profile of the rotation about the X axis of a number of optics on the sub-bench resulting from a 1° C external stimulus.

### 4.1 Dispersion

In order to meet the required maximum static spectral dispersion of 30 nm per single instrument pass there have been two design strategies. The first strategy is to minimize the dispersion of each optical component in the beam train. This approach is ultimately limited by technology capability and results in many constraints in component selection. Another strategy is to design the combiner in a "balanced" architecture. In a balanced combiner the separate optical paths of the interferometer are matched not only in geometric path length but in dispersive elements as well. In such a design the separate paths must be matched in bulk glass transmission, optical coatings and angles of incidence. In principle a balanced architecture results in a wavelength dependent phase dispersion that is identically zero. However, the presence of optics fabrication errors and alignment errors introduces imbalances in the system. Thus in a balanced architecture the non-zero static dispersion is limited by these errors.

The core beam combiner optical layout is schematically represented in Figure 5 where for simplicity only the main beam splitter, auxiliary beam splitters and compensator plates are shown. There are two ports that can be used for both retro source launch and fringe detection. Consequently, there are four possible configurations using this core design. For each of the four possible configurations one can trace the optical path of dispersing elements for each arm of the interferometer and determine whether the combined fringe output is balanced in phase. To do this one must add up the wavelength dependent phase contributions of all optical elements such as glass transmissions, transmission and reflection off of optical coatings. The results of this dispersion "book-keeping" are concisely summarized in Table 1. In this table the following notation is used. $T_{50}$ ($R_{50}$) denote a transmission (reflection) through a 50/50 power beam splitter. G denotes a single pass transmission through a substrate of glass. TAR denotes a transmission through an AR coating. We assume here that all beam splitter and anti-reflection coatings are identical, i.e. fabricated within the same deposition run. For simplicity we also ignore the differences between internal and external reflections. If one draws the distinction between these two the same result is obtained.

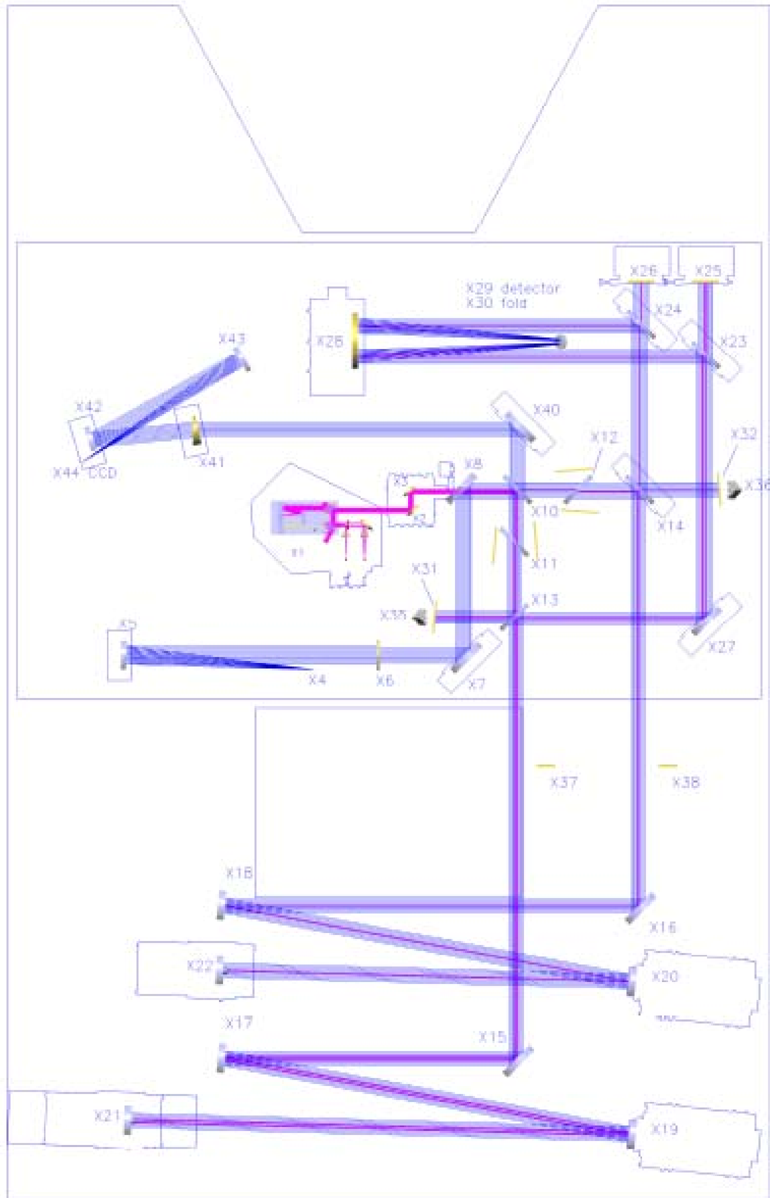


**Figure 4.** Layout of the spectral calibration development unit.

The table shows that in this layout there is only one configuration that is balanced in dispersion, namely the configuration in which Port B is employed to both launch the retro-mode light and to combine the light from the two arms. It is noteworthy that dispersion balance *is not* likewise attained in the configuration in which launch and detection are both implemented in Port A. This is due to the choice of orientation of the MBS. Although the layout may appear symmetric in the two ports, it is not. The symmetry is broken by the orientation of the MBS whose first and second surfaces have different coatings, one beam splitter coating and the other an anti-reflection coating. Regardless of the choice of input port, fringes can be observed in either or both of the two output ports. In the SIM flight instrument fringes will be simultaneously detected at both ports to maximize the intensity of collected light. From Table 1 we see that if the light is launched from Port B then the fringes observed in Port B will be balanced in phase dispersion whereas the fringes in Port A will not in general be balanced. However, if all coatings in the combiner are lossless (all dielectric layers) then by the principle of conservation of energy the fringes at Port A must also be balanced modulo a constant factor of pi radians.

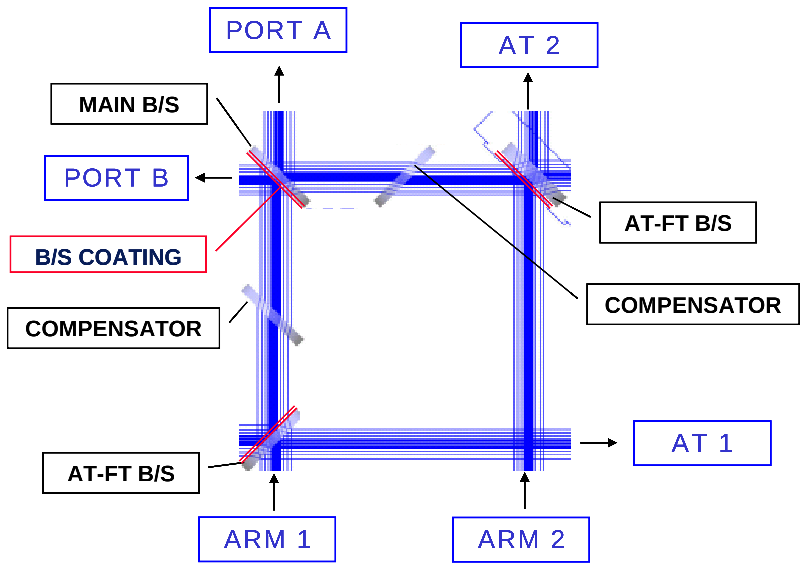


**Figure 5.** Schematic of the SCDU "balanced" beam combiner core. AT and FT denote angle tracker and fringe tracker cameras, respectively. The orientation of the coated surfaces of the optics is important.

| | INPUT PORT (SOURCE) | OUTPUT PORT (FT) | ARM 1 | | ARM 2 | No. OF B/S COATING PASSES |
|---|---|---|---|---|---|---|
| | A | A | $G^6 T_{AR}^8 T_{50}^4$ | ≈ | $R_{50}^4 G^6 T_{AR}^8$ | 4 |
| | A | B | $R_{50}^1 G^5 T_{AR}^7 T_{50}^3$ | ≈ | $R_{503}^3 G^5 T_{AR}^7 T_{50}^1$ | 4 |
| SCDU | B | A | $R_{50}^1 G^5 T_{AR}^7 T_{50}^3$ | ≈ | $R_{50}^3 G^5 T_{AR}^7 T_{50}^1$ | 4 |
| | B | B | $R_{50}^2 G^4 T_{AR}^6 T_{50}^2$ | = | $R_{50}^2 G^4 T_{AR}^6 T_{50}^2$ | 4 |

**Table 1.** The symbolic expressions of the net phase of each arm according to the input and output ports used in the combiner shown in Figure 5. The shaded row is the configuration to be used in SCDU.

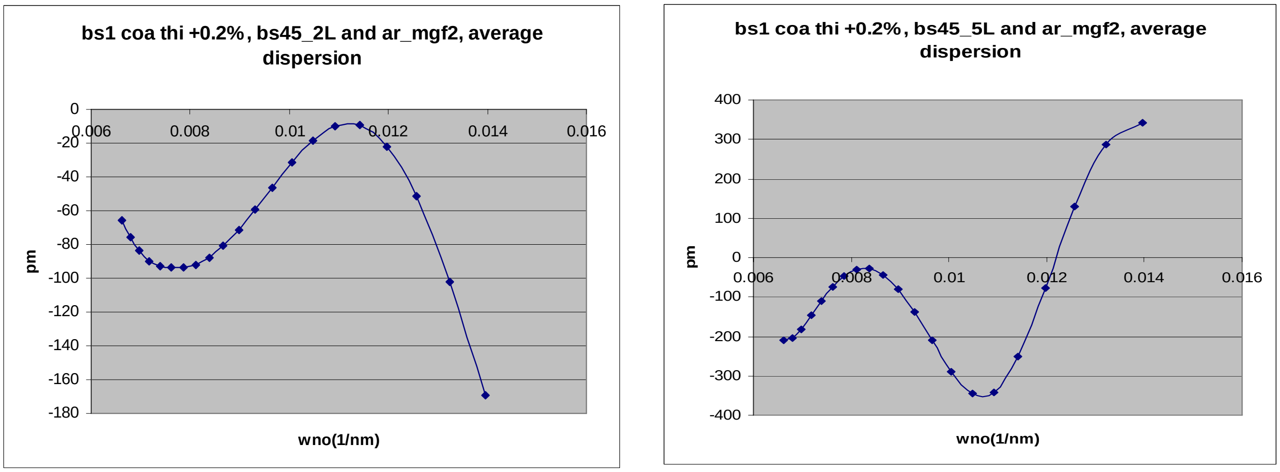


**Figure 6.** Predicted dispersion due to a fabrication error in coating layer thickness matching. The coating layers of beam splitter 1 (BS1) are perturbed in thickness by +0.2% for two cases. On the left, a 2-layer coating design; on the right, a 5-layer coating design.

### 4.2 Polarization

The required 100 pm of allowed retardance is more difficult to attain than the 30nm of dispersion. To attain this performance one must employ the most precise alignment procedure and coating deposition techniques to balance the retardance in the two arms as much as possible. The CODE V model of the combiner was used to predict the retardance due to coating thickness layer mismatch. The predicted retardances for two coating designs are shown in Figure 7. The two layer beam splitter coating has a clear advantage over the five layer. The disadvantage of the two layer coating is that it is impossible to achieve exactly 50% power separation. The best that can be achieved with two layers is approximately 60/40% whereas the five layer coating approaches 50/50.

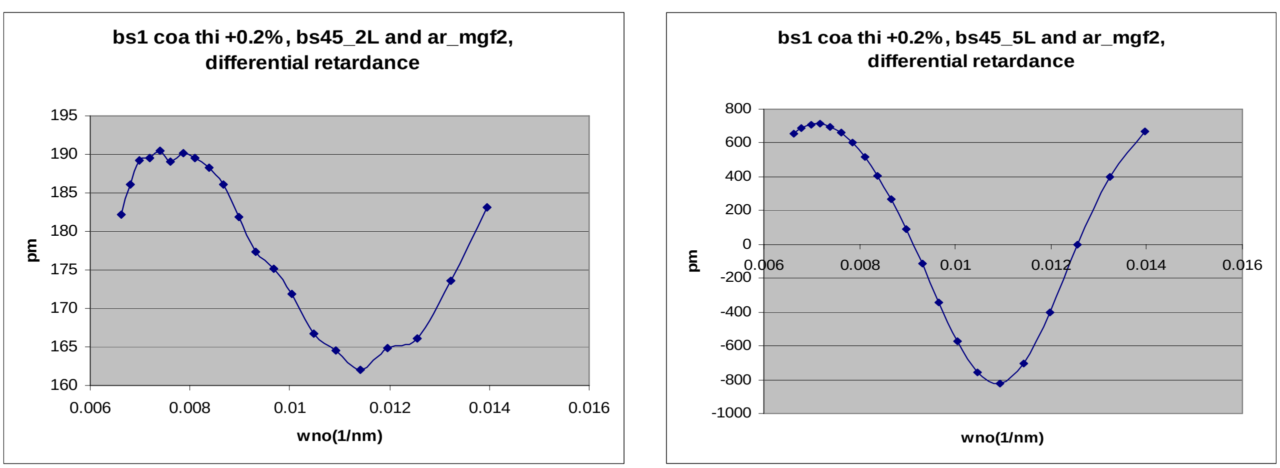


**Figure 7.** Predicted retardance due to a fabrication error in coating layer thickness matching. The coating layers of beam splitter 1 (BS1) are perturbed in thickness by +0.2% for two cases. On the left, a 2-layer coating design; on the right, a 5-layer coating design.

## CONCLUSION

The methodical design of the SCDU apparatus is intended to pathfind a wavelength calibration process for the SIM flight instrument. The development of such hardware for the demonstration of color calibration with picometer level accuracy and stability requires special design incorporating state of the art coatings, alignment procedures and data processing.


## ACKNOWLEDGEMENTS

The research described in this publication was performed at the Jet Propulsion Laboratory of the California Institute of Technology, under contract with the National Aeronautics and Space Administration. The authors would like to thank the entire SCDU team as well as contributing SIM team members for their contribution to the project.


[1] R. Goullioud and T. J Shen, "MAM testbed detail description and alignment", IEEE Aerospace Conference, March 6-13, 2004.